Research Square

Preprints are preliminary reports that have not undergone peer review.
They should not be considered conclusive, used to inform clinical practice,
or referenced by the media as validated information.

Association of Serum Uric Acid With Choroidal Thickness in Chronic Central Serous Chorioretinopathy: A Retrospective Exploratory Cohort Study

Yuman Wu[1]
The Affiliated Xuzhou Municipal Hospital of Xuzhou Medical University
Meili Li[1]
Institute of Eye Disease Prevention and Treatment of Xuzhou
Shuo Li[1]
Xuzhou First People's Hospital
Pengfei Duan[2]
Suqian Hospital of Nanjing Drum Tower Hospital Group
Yufeng Ma[1]
Xuzhou First People's Hospital
Sujuan Ji
13952180417@163.com
Xuzhou First People's Hospital
Xinting Wang
Institute of Eye Disease Prevention and Treatment of Xuzhou

Research Article

Keywords: central serous chorioretinopathy, uric acid, choroidal thickness, choroidal vascularity index, systemic biomarkers, subthreshold micropulse laser

Posted Date: November 1st, 2026

DOI: https://doi.org/10.21203/rs.3.rs-11317200/v1

License: This work is licensed under a Creative Commons Attribution 4.0 International License.
Read Full License

Additional Declarations: No competing interests reported.

Abstract

Background

To investigate associations between systemic biomarkers and quantitative choroidal phenotype in chronic central serous chorioretinopathy (cCSC), and to determine whether baseline serum uric acid (UA) is associated with early anatomical or functional recovery after subthreshold micropulse laser (SML).

Methods

This retrospective exploratory cohort included 47 patients with cCSC. Baseline blood testing comprised routine metabolic markers, blood-cell-derived inflammatory indices, and circulating cytokines. Best-corrected visual acuity (BCVA), contrast sensitivity (logCS), central macular thickness (CMT), subretinal fluid (SRF), central 0-3-mm choroidal vascularity index (CVI), and central 0-3-mm choroidal thickness (SCT) were assessed at baseline, day 7, and day 30. Baseline biomarker-SCT screening used age- and sex-adjusted linear regression with HC3 robust standard errors and Benjamini-Hochberg false-discovery-rate (FDR) correction. Early recovery models evaluated follow-up outcomes as a function of baseline UA while adjusting for the corresponding baseline ocular value, age, and sex; FDR correction was applied across 12 UA-follow-up tests.

Results

Mean age was 42.4 ± 5.7 years and 38/47 participants were men. UA was the only screened biomarker associated with baseline SCT after FDR correction (adjusted β = -0.840 μm per μmol/L, 95% CI -1.254 to -0.426; P < 0.001; q = 0.0023). At day 30, higher baseline UA was nominally associated with greater residual CMT (β = 30.5 μm per 100 μmol/L, 95% CI 4.8 to 56.3; P = 0.0199), but the association did not survive FDR correction (q = 0.239). The corresponding association with day-30 SRF was directionally similar but non-significant (β = 26.6 μm per 100 μmol/L; P = 0.064). No robust UA association was observed with BCVA, logCS, CVI, SCT, or complete SRF resolution.

Conclusions

Higher serum UA was associated with a thinner baseline central choroid in this exploratory cCSC cohort, but UA did not show robust evidence as an early SML response predictor. These findings support a potential systemic metabolic-choroidal relationship while emphasizing the distinction between baseline phenotype and treatment response.

Trial registration:

Not applicable.

Background

Central serous chorioretinopathy (CSC) is a chorioretinal disorder characterized by serous neurosensory retinal detachment and is increasingly considered within the pachychoroid disease spectrum [1, 2]. Choroidal venous congestion, hyperpermeability, pachyvessels, altered choriocapillaris perfusion, and increased choroidal thickness are central components of contemporary disease models [1–5]. Quantitative choroidal measures, including choroidal thickness and the choroidal vascularity index (CVI), have therefore become important imaging phenotypes for describing disease activity and treatment-related structural change [3, 6–8].

CSC is not solely an ocular vascular disorder. Epidemiologic and mechanistic studies have implicated corticosteroid exposure, hypertension, hypothalamic-pituitary-adrenal axis activation, endothelial dysfunction, systemic inflammation, and oxidative stress [9–16]. Blood-based studies have reported altered cytokine profiles, lipocalin-2, redox biomarkers, and metabolomic signatures in CSC [13–16, 29]. These findings raise the possibility that interindividual differences in the choroidal phenotype may partly reflect systemic metabolic or inflammatory states.

Serum uric acid (UA) is relevant to this question because it is linked to oxidative and endothelial pathways [18, 19]. In a population-based swept-source OCT study, higher serum UA was independently associated with a thinner macular choroid [17]. Whether this relationship is also present within cCSC is uncertain because CSC is itself characterized by a thick and hemodynamically abnormal choroid. Moreover, even if UA is associated with baseline choroidal structure, it does not necessarily follow that UA predicts subsequent fluid resolution or visual recovery.

Treatment provides an opportunity to separate these questions. SML can reduce SRF and central retinal thickness in CSC, although its effects on choroidal thickness, CVI, and perfusion are heterogeneous across studies [6, 8, 20–24]. We therefore investigated two related but distinct questions: (1) whether baseline systemic biomarkers are associated with quantitative choroidal phenotype in cCSC, and (2) whether baseline UA, if identified as a principal baseline signal, is associated with early anatomical or functional recovery after SML. All biomarker analyses were considered exploratory.

Methods

Study design and participants

This retrospective, single-centre exploratory cohort included 47 patients with cCSC treated at the Department of Ophthalmology, Xuzhou First People's Hospital, China, between July 2025 and May 2026. One treated eye per patient was analysed. Clinical records and examination data obtained at baseline (T0), day 7 (T7), and day 30 (T30) were retrospectively reviewed. The analysis was restricted to the first

30 days after the initial SML treatment because some patients subsequently underwent additional treatment, which could confound longer-term response assessment.

Inclusion criteria were age 18–50 years, fluorescein-angiographic findings characteristic of CSC, disease duration ≥ 3 months, macular SRF on optical coherence tomography (OCT), and no previous SML. Exclusion criteria were previous macular laser treatment, photodynamic therapy, or intravitreal anti-vascular endothelial growth factor therapy; choroidal neovascularization or other retinal disorders affecting macular structure or visual function, including age-related macular degeneration, diabetic retinopathy, and retinal vein occlusion; high myopia (spherical equivalent refractive error ≤ -6.00 D) or myopia-related macular abnormalities; uveitis, macular hole, or epiretinal membrane; media opacity preventing reliable fundus imaging; severe OCT artefacts or segmentation errors; and incomplete follow-up or examination data. The analytic cohort comprised patients with available baseline blood testing and complete ophthalmic measurements at T0, T7, and T30.

Subthreshold micropulse laser treatment

All study eyes underwent SML using the Smart532 laser system (Lumenis, USA) in SmartPulse subthreshold mode. Treatment parameters were: wavelength, 532 nm; power, 320 mW; spot diameter, 200 μm; exposure duration, 20 ms per spot; duty cycle, 5%; spot spacing, 0.25 × the spot diameter; and a 5 × 5 array pattern. The treatment area was individually determined according to fundus fluorescein angiography and swept-source OCT findings. Areas of retinal pigment epithelium abnormality and leakage associated with SRF were included in the treatment field. The number of array applications and total number of laser spots varied according to lesion size and treatment area. All procedures were performed by the same experienced retinal specialist.

Blood sampling and systemic biomarkers

Peripheral venous blood was obtained at T0 before treatment. Routine haematologic testing was performed in the central clinical laboratory of Xuzhou First People's Hospital using the BC-7500 automated haematology line, and routine biochemical testing was processed through the hospital's Remisol-linked automated biochemistry line, as recorded on the clinical laboratory reports. Variables included absolute neutrophil, lymphocyte, monocyte, and eosinophil counts; platelet count; alanine aminotransferase; γ-glutamyl transferase; UA; glucose; total cholesterol; triglycerides; high-density lipoprotein cholesterol; low-density lipoprotein cholesterol; and apolipoprotein B. Cytokine values available in the baseline clinical laboratory dataset included IL-1β, IL-2, IL-4, IL-5, IL-6, IL-8, IL-10, IL-12, IL-17, IFN-α, IFN-γ, and TNF-α. Laboratory values were analysed as continuous variables.

Derived inflammatory and metabolic indices were calculated as follows: neutrophil-to-lymphocyte ratio (NLR) = neutrophils/lymphocytes; platelet-to-lymphocyte ratio (PLR) = platelets/lymphocytes; monocyte-to-lymphocyte ratio (MLR) = monocytes/lymphocytes; systemic immune-inflammation index (SII) =

platelets × neutrophils/lymphocytes; monocyte-to-HDL-C ratio (MHR) = monocytes/HDL-C; and TG/HDL-C ratio = triglycerides/HDL-C. In total, 32 biomarkers or derived indices entered the baseline screening analysis.

Ophthalmic examinations and outcomes

Ophthalmic assessments were performed at T0, T7, and T30. BCVA was measured monocularly at 5 m using a standard logarithmic tumbling-E visual acuity chart under standardized illumination and converted to logarithm of the minimum angle of resolution (logMAR) units. Contrast sensitivity was assessed monocularly at 40 cm under standardized illumination using a POLYSH numeral contrast-sensitivity chart (SJ-108 series; Shengjue [Shanghai] Technology Co., Ltd., Shanghai, China). Each chart comprised 48 numerals arranged in eight rows of six, with contrast decreasing from higher to lower levels in 0.04-log-unit steps. Three alternate chart forms with different numeral sequences were used, one at T0, one at T7, and one at T30, to reduce recall of the numeral sequence. Participants read the numerals from left to right and from the highest to the lowest contrast. Testing was terminated after consecutive identification errors in accordance with the manufacturer's instructions, and the value corresponding to the last correctly identified numeral was recorded as a positive log contrast-sensitivity score (logCS), with higher values indicating better contrast sensitivity. Viewing distance, illumination, and the testing procedure were kept constant across visits.

Swept-source OCT/OCTA imaging was performed using the VG200D system (SVision Imaging, China). A 29 × 24-mm wide-field Angio scan was acquired with 1536 × 1280 sampling and a scan depth of 6.3 mm; the central 6 × 6-mm macular region centred on the fovea was used for quantitative analysis. CMT was the device-derived central macular thickness. SRF height was defined as the maximum vertical distance between the outer boundary of the neurosensory retina and the retinal pigment epithelium in the foveal region. Automated retinal and choroidal segmentations were reviewed at every visit and corrected when necessary before quantitative values were recorded.

CVI and SCT were quantified using the device's built-in ETDRS-based choroidal analysis with the grid centred on the fovea. The central 0-3-mm metric was derived from five ETDRS subfields: the central 0-1-mm subfield (C) and the superior, inferior, nasal, and temporal quadrants of the 1-3-mm inner ring (S, I, N, and T). Because each 1-3-mm quadrant has twice the area of the central 0-1-mm circle, area-weighted values were calculated as $[C + 2(S + I + N + T)]/9$ for both CVI and SCT. CVI was analysed as the device-derived vascular fraction for the selected choroidal volume and should not be interpreted as directly interchangeable with conventional two-dimensional ImageJ-derived CVI values. Sixteen study eyes were randomly selected for repeat SCT and CVI measurements at all three visits (48 paired OCT datasets).

Statistical analysis

Continuous variables are presented as mean ± standard deviation or median (interquartile range), as appropriate. Longitudinal ocular outcomes were evaluated with Friedman tests and Holm-adjusted

Wilcoxon signed-rank tests for pairwise comparisons. For the baseline phenotype analysis, each of the 32 systemic biomarkers or derived indices was entered separately into a linear regression model for central 0-3-mm SCT adjusted for age and sex. HC3 heteroskedasticity-consistent standard errors were used for inference in all baseline screening models, and Benjamini-Hochberg FDR correction was applied across the 32 tests. The only FDR-significant signal, the UA-SCT association, was then characterized using unadjusted, age-adjusted, sex-adjusted, principal age-and-sex-adjusted, and deliberately parsimonious sensitivity models, including a male-only analysis and exclusion of influential observations defined by Cook's distance > 4/n. Complete baseline screening results are provided in Additional file 1: Table S1.

To assess early treatment response, ANCOVA-style models were used rather than simple change-score correlations. Each T7 or T30 ocular outcome was modelled as a function of baseline UA, the corresponding baseline ocular value, age, and sex, using HC3 robust standard errors. Twelve UA-follow-up tests were evaluated (six ocular outcomes at two time points), and Benjamini-Hochberg FDR correction was applied across these 12 tests. UA coefficients in all follow-up models were expressed per 100 μmol/L higher serum UA for clinical interpretability. Complete model results are provided in Additional file 1: Table S2.

Complete SRF resolution was defined as SRF = 0 μm. Because only eight eyes had complete resolution at T7, this time point was summarized descriptively and no multivariable logistic model was fitted. At T30, complete SRF resolution was examined using logistic regression with baseline UA (per 100 μmol/L), baseline SRF, age, and sex as predictors. A broader exploratory screen evaluated all 32 baseline biomarkers against each of the six T7 and T30 ocular outcomes using the same baseline-adjusted model structure and HC3 robust standard errors; FDR correction was applied separately within each 32-test outcome-time family (Additional file 1: Table S3).

Missing data were handled by complete-case analysis without imputation. Reproducibility was quantified using ICC(2,1), a two-way random-effects, absolute-agreement, single-measurement model. Eye-level cluster bootstrap resampling (3,000 replicates) preserved within-eye clustering across visits when deriving 95% confidence intervals for ICC estimates. Analyses were performed using R 4.5.1 and Python 3.13.

Use of AI-assisted language tools

AI-assisted tools were used only for English translation and language polishing without changing the intended scientific meaning. All edited text, statistical values, references, and interpretations were reviewed and verified by the authors, who take full responsibility for the final manuscript.

Ethics approval

The study protocol was approved by the Ethics Review Committee of Xuzhou First People's Hospital (approval no. xyyll[2026]177; August 3, 2026). The requirement for informed consent was waived by the

ethics committee because the study involved retrospective analysis of existing clinical data. The study was conducted in accordance with the Declaration of Helsinki and its subsequent amendments.

Results

Cohort characteristics and longitudinal ocular changes

The cohort comprised 47 patients (38 men, 9 women) with a mean age of 42.4 ± 5.7 years. Baseline median SCT was 477.6 μm (IQR 411.6-556.9), median CVI was 0.408 (0.381–0.429), and mean UA was 342.7 ± 79.4 μmol/L (Table 1). Significant overall changes occurred in BCVA (P = 0.002), CMT, SRF, logCS, and SCT (all P < 0.001 except BCVA) across T0, T7, and T30, whereas CVI did not show a significant overall longitudinal change (P = 0.059) (Table 2). At T30, median SRF had decreased to 23 μm (IQR 0-115), and 23/47 eyes (48.9%) had complete SRF resolution.

Table 1
Baseline demographic, ocular, and selected systemic characteristics

Characteristic	Value
Age, years	42.4 ± 5.7
Male sex, n (%)	38 (80.9)
BCVA, logMAR	0.200 (0.098–0.400)
Contrast sensitivity, logCS	1.240 (1.100–1.440)
CMT, μm	326.0 (272.2–400.5)
SRF height, μm	128.0 (91.0–195.5)
Central 0–3-mm SCT, μm	477.6 (411.6–556.9)
Central 0–3-mm CVI	0.408 (0.381–0.429)
Uric acid, μmol/L	342.7 ± 79.4
Glucose, mmol/L	5.67 (5.29–6.66)
Total cholesterol, mmol/L	5.18 ± 0.96
Triglycerides, mmol/L	2.19 (1.31–3.91)
HDL-C, mmol/L	1.26 (1.11–1.55)
LDL-C, mmol/L	2.86 ± 0.59
ApoB, g/L	0.92 ± 0.19
NLR	2.21 (1.73–2.69)
PLR	126.8 (99.2–146.9)
MLR	0.21 (0.16–0.25)
SII	505.3 (380.7–615.9)

Values are mean ± SD or median (IQR), unless otherwise indicated.

Table 2
Longitudinal ocular outcomes at baseline, day 7, and day 30

Parameter	T0	T7	T30	Overall P	T0 vs T7	T0 vs T30	T7 vs T30
BCVA (logMAR)	0.200 (0.098–0.400)	0.200 (0.098–0.351)	0.200 (0.098–0.301)	0.002	0.022	0.009	0.041
CMT (μm)	326.0 (272.2–400.5)	294.8 (224.5–382.0)	254.0 (191.0–337.4)	< 0.001	< 0.001	< 0.001	< 0.001
SRF (μm)	128.0 (91.0–195.5)	91.0 (49.5–204.0)	23.0 (0–115.0)	< 0.001	< 0.001	< 0.001	< 0.001
logCS	1.240 (1.100–1.440)	1.400 (1.260–1.480)	1.480 (1.380–1.600)	< 0.001	< 0.001	< 0.001	< 0.001
CVI	0.408 (0.381–0.429)	0.424 (0.394–0.453)	0.421 (0.384–0.453)	0.059	0.012	0.354	0.354
SCT (μm)	477.6 (411.6–556.9)	464.3 (401.7–548.6)	460.6 (373.1–531.9)	< 0.001	0.171	< 0.001	0.002

Overall P values are from Friedman tests; pairwise P values are Holm-adjusted Wilcoxon signed-rank tests.

Systemic biomarkers and baseline choroidal thickness

Among the 32 baseline biomarkers and derived indices, UA was the only marker associated with baseline SCT after age/sex adjustment, HC3 robust inference, and FDR correction (β = -0.840 μm per μmol/L, 95% CI -1.254 to -0.426; P < 0.001; q = 0.0023; Fig. 1). The crude association was weaker (β = -0.390; P = 0.068), primarily because men had both higher UA and thicker choroids. Adjustment for sex strengthened the inverse association (Table 3). The result remained stable after additional adjustment for available metabolic covariates, in the male-only analysis, and after exclusion of influential observations. Intra-grader reproducibility was excellent for SCT (ICC = 0.996, cluster-bootstrap 95% CI 0.976-1.000) and CVI (ICC = 0.991, 95% CI 0.965–0.999). Complete results for all 32 baseline screening models are provided in Additional file 1: Table S1.

Table 3
Association between baseline serum uric acid and baseline central 0-3-mm choroidal thickness

Model	n	UA β (μm/μmol/L)	95% CI	P
Unadjusted	47	-0.390	-0.809 to 0.028	0.068
Age adjusted	47	-0.547	-0.989 to -0.105	0.015
Sex adjusted	47	-0.766	-1.163 to -0.370	< 0.001
Age + sex (principal model)	47	-0.840	-1.254 to -0.426	< 0.001
Age + sex + TC + glucose	47	-0.981	-1.387 to -0.576	< 0.001
Age + sex + TC + glucose + GGT	47	-0.956	-1.451 to -0.460	< 0.001
Men only, + age	38	-0.931	-1.413 to -0.450	< 0.001
Cook's distance ≤ 4/n	44	-0.854	-1.289 to -0.419	< 0.001

The age- and sex-adjusted UA-SCT association was the only signal remaining significant after FDR correction across 32 baseline biomarker tests (q = 0.0023). HC3 robust standard errors were used for inference.

Figure 1. Relationship between serum uric acid and baseline central 0-3-mm choroidal thickness stratified by sex. Sex-stratified visualization is shown to illustrate attenuation of the crude pooled association by between-sex differences in both uric acid and choroidal thickness. Formal inference is based on the multivariable regression models in Table 3.

Baseline uric acid and early treatment response

Baseline UA was not associated with any T7 ocular outcome after adjustment for the corresponding T0 value, age, and sex (Table 4). At T30, higher UA was nominally associated with greater residual CMT: each 100 μmol/L higher UA corresponded to 30.5 μm greater T30 CMT (95% CI 4.8 to 56.3 μm; P = 0.0199). However, this association did not remain significant after FDR correction across the 12 UA-follow-up tests (q = 0.239). T30 SRF showed a directionally similar but non-significant association (+ 26.6 μm per 100 μmol/L UA; 95% CI -1.5 to 54.7; P = 0.064; q = 0.382). No significant adjusted association was observed between UA and T30 BCVA, logCS, CVI, or SCT. Complete results are provided in Additional file 1: Table S2.

Table 4
Baseline serum uric acid and early post-treatment ocular outcomes

Time	Outcome	n	β per 100 μmol/L UA	95% CI	P	FDR q
T7	BCVA (logMAR)	47	0.0175	-0.0099 to 0.0450	0.211	0.561
T30	BCVA (logMAR)	47	0.0138	-0.0147 to 0.0422	0.343	0.685
T7	CMT (μm)	47	-15.1	-66.8 to 36.6	0.567	0.935
T30	CMT (μm)	47	30.5	4.8 to 56.3	0.0199	0.239
T7	SRF (μm)	47	-5.6	-58.4 to 47.1	0.834	0.935
T30	SRF (μm)	47	26.6	-1.5 to 54.7	0.064	0.382
T7	logCS	47	-0.0272	-0.0713 to 0.0168	0.225	0.561
T30	logCS	47	-0.0266	-0.0703 to 0.0172	0.234	0.561
T7	CVI	47	0.00351	-0.02117 to 0.02818	0.781	0.935
T30	CVI	47	0.00232	-0.02108 to 0.02572	0.846	0.935
T7	SCT (μm)	47	-1.16	-13.81 to 11.48	0.857	0.935
T30	SCT (μm)	47	0.52	-13.90 to 14.94	0.944	0.944

Each model adjusted for the corresponding baseline ocular value, age, and sex and used HC3 robust standard errors. UA coefficients are expressed per 100 μmol/L higher UA. FDR q values are Benjamini-Hochberg adjusted across the 12 UA-follow-up tests. No association remained significant after FDR correction.

Complete SRF resolution occurred in 8/47 eyes (17.0%) at T7 and 23/47 eyes (48.9%) at T30. Because only eight T7 events were observed, no adjusted logistic model was fitted at that time point. At T30, higher baseline UA was not significantly associated with complete SRF resolution after adjustment for baseline SRF, age, and sex (OR = 0.60 per 100 μmol/L, 95% CI 0.19–1.87; P = 0.378). In the broader 32-biomarker recovery screen, 17 nominal $P < 0.05$ associations were observed across T7/T30 outcomes, but none survived FDR correction. Thus, no baseline systemic biomarker met multiplicity-controlled criteria as an early treatment-response marker (Additional file 1: Table S3).

Discussion

In this exploratory cCSC cohort, the principal systemic signal was an inverse association between serum UA and baseline central choroidal thickness. This association survived multiplicity correction and remained stable in parsimonious sensitivity analyses. In contrast, when the same baseline UA measurement was tested against subsequent anatomical and functional outcomes, no association

survived FDR correction. The distinction is important: the present data support UA as a correlate of baseline choroidal phenotype, but not as a validated predictor of early SML response.

The UA-SCT finding is directionally consistent with population-based swept-source OCT data showing thinner macular choroid with higher UA [17]. UA has complex redox biology and has been associated with endothelial dysfunction in systemic vascular disease [18, 19]. In CSC, where choroidal venous congestion and endothelial/perfusion abnormalities are central to current pathophysiologic models [1, 2, 4, 5, 12], a systemic metabolic correlate of choroidal thickness is biologically plausible. Nevertheless, the present association cannot establish mechanism. UA may be a marker of broader metabolic or vascular states rather than a direct determinant of choroidal structure.

The sex-related attenuation of the crude association deserves emphasis. Men in this cohort had both higher UA and thicker choroids, creating a group-level pattern that weakened the inverse within-cohort relationship. The association became stronger after sex adjustment and remained significant in the male-only sensitivity analysis. This pattern supports appropriate covariate control but does not eliminate residual confounding. The female subgroup was small, and important determinants of UA and choroidal thickness-including axial length, body mass index, blood pressure, renal function, and standardized imaging time-were unavailable [25–28].

The longitudinal analysis addresses a separate clinical question. Higher UA was nominally associated with greater residual CMT at T30 and showed the same unfavorable direction for residual SRF, but the CMT association did not survive multiplicity correction and complete SRF resolution was not significantly associated with UA. Accordingly, it would be inappropriate to describe UA as a treatment-response biomarker. This negative distinction is informative because baseline structural correlates need not predict dynamic response to therapy. SML studies have likewise shown that SRF, retinal thickness, choroidal thickness, CVI, and perfusion indices may change on different time scales and do not necessarily move in parallel [6–8, 20–24].

The absence of robust inflammatory or cytokine response markers is also relevant. Prior studies have reported altered plasma cytokines, lipocalin-2, inflammatory ratios, metabolomic profiles, and oxidative stress markers in CSC [13–16, 29, 30]. Such studies support systemic involvement but have produced heterogeneous candidate biomarkers. In the present dataset, broad screening generated several nominal associations with early ocular outcomes, but none survived FDR correction. This reinforces the need for multiplicity control in small exploratory biomarker studies and argues against selecting isolated P values as clinical predictors.

Strengths of this study include concurrent systemic biomarker profiling and quantitative choroidal imaging, repeated ocular assessment, explicit separation of baseline phenotype from treatment response, multiplicity control, robust regression, sensitivity analyses, and excellent intra-grader reproducibility of SCT and CVI. Limitations include the modest sample size, retrospective single-centre design, absence of a healthy control group, short 30-day follow-up, and incomplete systemic and ocular confounder assessment. Treatment-response analyses were exploratory and underpowered for modest

effects. Repeatability was intra-grader rather than inter-grader. The broad biomarker panel also increases the possibility of unstable nominal signals despite FDR control. In addition, the device-derived volumetric CVI metric used here is not directly interchangeable with conventional two-dimensional binarization-derived CVI values.

Conclusions

Higher serum UA was associated with a thinner central choroid in patients with cCSC after adjustment for age and sex and correction for multiple testing. However, baseline UA did not robustly predict early anatomical or functional recovery after SML. These findings suggest that UA may be more informative as a systemic correlate of choroidal phenotype than as a short-term treatment-response marker. Prospective studies with larger cohorts, longer follow-up, healthy or disease controls, and comprehensive assessment of axial length, renal function, blood pressure, body composition, and diurnal imaging effects are required.

Abbreviations

ALT
alanine aminotransferase
ApoB
apolipoprotein B
BCVA
best-corrected visual acuity
CMT
central macular thickness
CSC
central serous chorioretinopathy
cCSC
chronic central serous chorioretinopathy
CVI
choroidal vascularity index
FDR
false discovery rate
GGT
γ-glutamyl transferase
HDL-C
high-density lipoprotein cholesterol
ICC
intraclass correlation coefficient
IFN
interferon

IL
interleukin
IQR
interquartile range
LDL-C
low-density lipoprotein cholesterol
logCS
logarithmic contrast sensitivity
logMAR
logarithm of the minimum angle of resolution
MHR
monocyte-to-HDL-C ratio
MLR
monocyte-to-lymphocyte ratio
NLR
neutrophil-to-lymphocyte ratio
OCT
optical coherence tomography
OCTA
optical coherence tomography angiography
PLR
platelet-to-lymphocyte ratio
RPE
retinal pigment epithelium
SCT
choroidal thickness
SII
systemic immune-inflammation index
SML
subthreshold micropulse laser
SRF
subretinal fluid
TC
total cholesterol
TG
triglycerides
UA
uric acid.

Declarations

Ethics approval and consent to participate

The study protocol was approved by the Ethics Review Committee of Xuzhou First People's Hospital (approval no. xyyll[2026]177; August 3, 2026). The requirement for informed consent was waived by the ethics committee because the study involved retrospective analysis of existing clinical data. The study was conducted in accordance with the Declaration of Helsinki and its subsequent amendments.

Consent for publication

Not applicable. No identifiable individual participant data or images are included in this manuscript.

Competing interests

The authors declare no competing interests.

Additional files

Additional file 1: XLSX. Supplementary Tables. Table S1: age- and sex-adjusted associations of 32 baseline systemic biomarkers and derived indices with baseline central 0-3-mm SCT, using HC3 robust standard errors and Benjamini-Hochberg FDR correction. Table S2: baseline UA associations with T7 and T30 ocular outcomes in baseline-adjusted ANCOVA-style models with HC3 robust standard errors and FDR correction across 12 tests. Table S3: broader exploratory screen of 32 baseline biomarkers against six ocular outcomes at T7 and T30, with FDR correction within each outcome-time family.

Funding

No funding or sponsorship was received for this study or publication.

Author Contribution

YW, XW, and SJ conceived the study and developed the methodology. YW, XW, ML, SL, PD, and YM collected and curated the data. YW performed the formal analysis and drafted the manuscript. SJ supervised the study. All authors critically revised the manuscript, approved the final version, and agree to be accountable for the work.

Acknowledgements

The authors thank the patients whose clinical data contributed to this study.

Data Availability

The datasets generated and/or analysed during the current study are available from the corresponding author on reasonable request. The data are not publicly available because they contain clinical information from human participants and are subject to institutional and ethical restrictions.

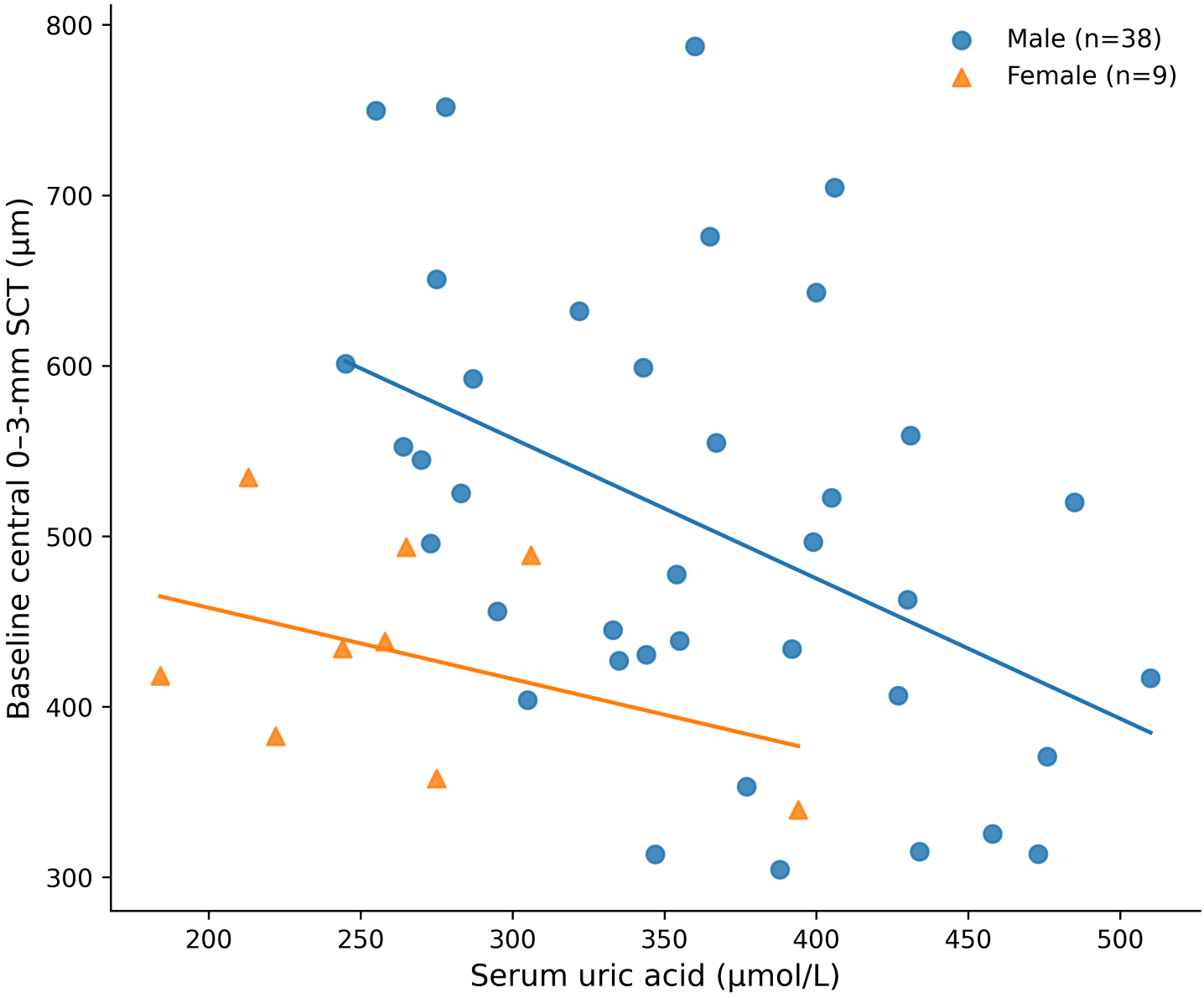
References

1. Cheung CMG, Dansingani KK, Koizumi H, et al. Pachychoroid disease: review and update. Eye. 2024. 10.1038/s41433-024-03253-4.
2. Kanda P, Noda K, Ishida S. Pathophysiology of central serous chorioretinopathy: a literature review with quality assessment. Eye (Lond). 2022;36:941–62. 10.1038/s41433-021-01808-3.
3. Singh SR, Iovino C, Zur D, et al. Central serous chorioretinopathy imaging biomarkers. Br J Ophthalmol. 2022;106:553–8. 10.1136/bjophthalmol-2020-317422.
4. Inferrera L, Marangoni D, Valastro A, et al. Choriocapillaris flow deficits and choroidal vascular index in the fellow eye of patients with central serous chorioretinopathy. Graefes Arch Clin Exp Ophthalmol. 2026;264:2019–29. 10.1007/s00417-026-07147-x.
5. Kabiri P, Künzel S, Ashraf-Vaghefi S, et al. Changes in choroidal vessel morphology associated with fluid leakage in central serous chorioretinopathy; a comparison of OCTA and ICGA. Graefes Arch Clin Exp Ophthalmol. 2025;263:3065–72. 10.1007/s00417-025-06918-2.
6. van Dijk EHC, Singh SR, Vupparaboina KK, et al. Prospective evaluation of changes in choroidal vascularity index after half-dose photodynamic therapy versus micropulse laser treatment in chronic central serous chorioretinopathy. Graefes Arch Clin Exp Ophthalmol. 2020;258:1191–7. 10.1007/s00417-020-04619-6.
7. Sevik MO, Aykut A, Çam F, Dericioğlu V, Şahin Ö. Choroidal vascularity index as an activity criterion and a treatment response measure in chronic central serous chorioretinopathy. Ophthalmic Physiol Opt. 2023;43:1203–10. 10.1111/opo.13187.
8. Yang X, Yan M, Song Y, et al. Quantitative choroidal evaluation after subthreshold micropulse laser in chronic central serous chorioretinopathy using ultrawide-field SS-OCTA. BMC Ophthalmol. 2026. 10.1186/s12886-026-05149-1.
9. Liu B, Deng T, Zhang J. Risk factors for central serous chorioretinopathy: a systematic review and meta-analysis. Retina. 2016;36:9–19.
10. Haimovici R, Koh S, Gagnon DR, Lehrfeld T, Wellik S. Risk factors for central serous chorioretinopathy: a case-control study. Ophthalmology. 2004;111:244–9.
11. van Haalen FM, van Dijk EHC, Dekkers OM, et al. Cushing's syndrome and hypothalamic-pituitary-adrenal axis hyperactivity in chronic central serous chorioretinopathy. Front Endocrinol (Lausanne). 2018;9:39.

12. Wang NK, Fu Y, Wang JP, et al. Peripheral vascular endothelial dysfunction in central serous chorioretinopathy. Invest Ophthalmol Vis Sci. 2017;58:4524–9. 10.1167/iovs.17-21825.
13. Karska-Basta I, Pociej-Marciak W, Chrząszcz M, et al. Altered plasma cytokine levels in acute and chronic central serous chorioretinopathy. Acta Ophthalmol. 2021;99:e222–31. 10.1111/aos.14547.
14. Matet A, Jaworski T, Bousquet E, et al. Lipocalin 2 as a potential systemic biomarker for central serous chorioretinopathy. Sci Rep. 2020;10:20175. 10.1038/s41598-020-77202-y.
15. Akıdan EE, Yılmaz E, Yılmaz N, Akıdan M. Increased oxidative stress biomarkers in central serous chorioretinopathy. Sci Rep. 2024;14:21099. 10.1038/s41598-024-71890-6.
16. Nkrumah G, Paez-Escamilla M, Singh SR, et al. Biomarkers for central serous chorioretinopathy. Ther Adv Ophthalmol. 2020;12:2515841420950846. 10.1177/2515841420950846.
17. Xiong K, Gong X, Xie L, et al. Influence of serum uric acid on macular choroidal thickness and ganglion cell inner plexiform layer thickness. Transl Vis Sci Technol. 2023;12:13. 10.1167/tvst.12.5.13.
18. Maruhashi T, Hisatome I, Kihara Y, Higashi Y. Hyperuricemia and endothelial function: from molecular background to clinical perspectives. Atherosclerosis. 2018;278:226–31. 10.1016/j.atherosclerosis.2018.10.007.
19. Khosla UM, Zharikov S, Finch JL, et al. Hyperuricemia induces endothelial dysfunction. Kidney Int. 2005;67:1739–42. 10.1111/j.1523-1755.2005.00273.x.
20. van Dijk EHC, Fauser S, Breukink MB, et al. Half-dose photodynamic therapy versus high-density subthreshold micropulse laser treatment in patients with chronic central serous chorioretinopathy: the PLACE trial. Ophthalmology. 2018;125:1547–55. 10.1016/j.ophtha.2018.04.021.
21. van Rijssen TJ, Hahn LC, van Dijk EHC, et al. Response of choroidal abnormalities to photodynamic therapy versus micropulse laser in chronic central serous chorioretinopathy: PLACE trial report 4. Retina. 2021;41:2122–31. 10.1097/IAE.0000000000003157.
22. Sun Z, Huang Y, Nie C, et al. Efficacy and safety of subthreshold micropulse laser compared with threshold conventional laser in central serous chorioretinopathy. Eye (Lond). 2020;34:1592–9. 10.1038/s41433-019-0692-8.
23. Zhou L, Huang C, Li Z, et al. A randomized non-inferiority trial of 577 nm subthreshold micropulse laser versus half-dose photodynamic therapy for acute central serous chorioretinopathy. Photodiagnosis Photodyn Ther. 2024;45:103908. 10.1016/j.pdpdt.2023.103908.
24. Li X, Long H, Hu Q. Efficacy of subthreshold micropulse laser for chronic central serous chorioretinopathy: a meta-analysis. Photodiagnosis Photodyn Ther. 2022;39:102931. 10.1016/j.pdpdt.2022.102931.
25. Ikuno Y, Kawaguchi K, Nouchi T, Yasuno Y. Choroidal thickness in healthy Japanese subjects. Invest Ophthalmol Vis Sci. 2010;51:2173–6. 10.1167/iovs.09-4383.
26. Tan CS, Ouyang Y, Ruiz H, Sadda SR. Diurnal variation of choroidal thickness in normal, healthy subjects measured by spectral domain optical coherence tomography. Invest Ophthalmol Vis Sci. 2012;53:261–6. 10.1167/iovs.11-8782.

27. Lee SW, Yu SY, Seo KH, Kim ES, Kwak HW. Diurnal variation in choroidal thickness in relation to sex, axial length, and baseline choroidal thickness in healthy Korean subjects. Retina. 2014;34:385–93. 10.1097/IAE.0b013e3182993f29.
28. Tuncer I, Karahan E, Zengin MO, Atalay E, Polat N. Choroidal thickness in relation to sex, age, refractive error, and axial length in healthy Turkish subjects. Int Ophthalmol. 2015;35:403–10. 10.1007/s10792-014-9962-4.
29. Xu H, Huang L, Jin E, Liang Z, Zhao M. Plasma metabolomic profiling of central serous chorioretinopathy. Exp Eye Res. 2021;203:108401. 10.1016/j.exer.2020.108401.
30. Sirakaya E, Duru Z, Kuçuk B, Duru N. Monocyte to high-density lipoprotein and neutrophil-to-lymphocyte ratios in patients with acute central serous chorioretinopathy. Indian J Ophthalmol. 2020;68:854–8. 10.4103/ijo.IJO_1327_19.

Figures



Male: Spearman ρ=-0.425, P=0.0078; Female: ρ=-0.283, P=0.460; UA×sex interaction P=0.617.

Figure 1

Relationship between serum uric acid and baseline central 0-3-mm choroidal thickness stratified by sex. Sex-stratified visualization is shown to illustrate attenuation of the crude pooled association by between-sex differences in both uric acid and choroidal thickness. Formal inference is based on the multivariable regression models in Table 3.

Supplementary Files

This is a list of supplementary files associated with this preprint. Click to download.

- Additionalfile1SupplementarTables.xlsx